14th International Conference on Structural Safety and Reliability - ICOSSAR'25
1-6 June, 2025 - Los Angeles California, USA
R. Ghanem, E. Johnson, S. Masri and A. Olivier (Eds)

RANDOM VIBRATIONS OF AXISYMMETRIC VISCOELASTIC NONLOCAL PLATES

Francesco P. Pinnola[1], **Francesco Scudieri**[1], **Gioacchino Alotta**[2], **Francesco Marotti de Sciarra**[1]

[1] University of Naples "Federico II"
Naples, 80125, Italy
francescopaolo.pinnola@unina.it, francesco.scudieri@unina.it, francesco.marotti@unina.it

[2] University of Reggio Calabria "Mediterranea"
Reggio Calabria, 89124, Italy
giacchino.alotta@unirc.it

Key words: Nano- and micro-plates, stress-driven nonlocal model, fractional-order viscoelasticity, stochastic dynamics

Abstract. The flexural vibrations of small-scale plates subjected to stochastic input are investigated. The dynamics of this problem is studied under the kinematic assumptions of the Kirchhoff axisymmetric model. This research is relevant to the design of bidimensional nano- and micro-structures used as energy harvesters, sensors, actuators, wave converters, components of transistors, bioinspired devices, small-scale robots, and similar applications. For these miniaturized structures, often made from unconventional materials, classical local elastic continuum theories fall short in providing accurate models. Therefore, their mechanical behavior is analyzed by considering two crucial aspects: viscoelasticity and nonlocality. The constitutive law employed is based on a stress-driven integral nonlocal model combined with fractional-order viscoelasticity. This approach captures both hereditary and size-dependent effects. The external dynamic loads are modeled by incorporating their stochastic nature to provide a more realistic representation of the system's conditions. Under these assumptions, the dynamics of this complex system in terms of time-dependent transversal displacement field is governed by a stochastic partial integro-differential equation incorporating fractional differential operators. Solving such an equation is computationally challenging. For this reason, a semi analytical procedure to solve this problem by means of a modal decomposition procedure, evaluating the steady-state response and providing results in terms of power spectra is proposed. Presented results show how geometry, nonlocal parameter and viscoelastic coefficients influence the mechanical response and the main frequencies of the structure. Numerical and theoretical outcomes can help in the design of sophisticated small-scale bi-dimensional devices.

1 INTRODUCTION

In recent decades, the field of constitutive modeling of materials has witnessed significant advancements. This progress has been driven by the need for mathematical models capable of accurately capturing the behavior of unconventional materials, as well as the specialized responses of conventional materials in unique engineering applications. These models are expected to strike a balance

between predictive accuracy and computational efficiency. Among the most rapidly evolving areas is *nonlocal mechanics*. Classical continuum theories often fail to predict the mechanical response of micro- and nanostructures due to pronounced size effects. Although molecular dynamics simulations provide high-fidelity representations of material behavior across scales, their computational cost frequently makes them impractical for large systems or long time spans. As a viable alternative, nonlocal theories extend classical continuum mechanics by incorporating long-range interactions and/or higher-order gradients into the governing equations. The strain-driven Eringen integral model (EIM) is among the first and most well-known nonlocal constitutive models[1, 2]. In this model, the stress field is obtained by convolving the elastic strain field with a suitable kernel function. In unbounded domains, this convolution leads to a first-kind Fredholm integral equation, which can be reformulated as a differential equation, known as the Eringen differential nonlocal model (EDM). This reformulation is convenient due to the implicit satisfaction of boundary conditions that vanish at infinity. However, when applied to bounded domains, EDM does not directly correspond to EIM, necessitating the introduction of appropriate strain-driven constitutive boundary conditions (CBC) for equivalence. Additionally, mathematical challenges and physical paradoxes arise in bounded domains [3, 4]. To address these issues, various alternative nonlocal approaches have been developed, including two-phase models [5], strain-difference approaches [6], strain and stress gradient theories [7], micropolar Cosserat theory [8], couple stress theory [9], peridynamics [10], displacement-based nonlocal models [11], fractional calculus-based models [12], and stress-driven integral formulations [13, 14].

Another key aspect of the constitutive behavior of unconventional materials is time dependence, often referred to as *viscoelasticity* or *hereditariness*. Viscoelastic materials exhibit mechanical memory, leading to stress relaxation under constant strain and strain accumulation under constant stress. Traditional models describe viscoelasticity through combinations of elastic (spring) and viscous (dashpot) elements. However, these models have limitations, particularly when compared to fractional viscoelasticity, which is based on extensive experimental evidence suggesting that stress relaxation and creep follow power laws [15]. In linear viscoelasticity, adopting power-law kernels in the Boltzmann superposition integrals results in constitutive laws involving fractional differential operators [16]. Fractional viscoelastic models are advantageous due to their ability to capture long-term memory effects and efficiently fit experimental data using fewer parameters [17].

This paper proposes a nonlocal viscoelastic model for circular Kirchhoff plates, suitable for simulating unconventional mechanical behaviors in various engineering applications. These include size effects at small scales [18], strain and stress localization [19], anomalous wave dispersion in complex materials with distinct microstructures [20], and structures influenced by long-range force fields [21, 22]. Additionally, the model is relevant for macro-scale engineering components, such as the elastomeric membranes of Wave Energy Converters (WECs). These membranes consist of alternating layers of elastomers and piezoelectric materials, with the latter converting wave energy into electricity. The elastomer layers necessitate a viscoelastic description, while the piezoelectric layers generate electric and magnetic fields that interact with membrane motion. Nonlocal interactions offer a simplified approach to modeling these effects, which are explicitly considered in other studies [23, 24].

For nonlocal behavior, this work adopts the stress-driven integral model, which has gained significant attention in solid mechanics due to its simplicity, well-posedness, and ability to yield analytical solutions for structural mechanics problems [25, 26, 27, 28]. The fractional Kelvin-Voigt model is selected to describe viscoelasticity, as it generalizes the classical Kelvin-Voigt model commonly used in dynamic analyses of viscoelastic structures. The nonlocal viscoelastic circular plate is considered

under stochastic loading, relevant for applications such as micro/nanosensors or WEC membranes. Numerical simulations illustrate how the nonlocal parameter, and viscoelastic coefficients influence mechanical responses and structural frequencies. The results provide valuable insights for designing advanced small-scale bi-dimensional devices.

2 NONLOCAL VISCOELASTIC AXISYMMETRIC PLATE

The dynamic problem of a homogeneous nonlocal viscoelastic moderate-thin circular plate with radius R and thickness h is introduced below.

2.1 Kinematics relations

The problem is formulated with respect to a cylindrical coordinate system (r, θ, z) centered at the centroid of the disk. Specifically, z is the vertical axis, while r and θ define the mid-plane of the plate. Denoting by $w(r, \theta, t)$ the evolution in time t of the vertical displacement of a generic point on the mid-plane, the displacement field $\mathbf{s}$ is expressed as:

$$\mathbf{s}(r, \theta, z, t) = \begin{pmatrix} s_r \\ s_\theta \\ s_z \end{pmatrix} = \begin{pmatrix} -z\,\partial_r w \\ -\dfrac{z}{r}\,\partial_\theta w \\ w \end{pmatrix} \tag{1}$$

where ∂_i denotes the partial derivative respect j-variable, s_r, s_θ and s_z are the radial, circumferential and transverse displacements, respectively. Under the assumption of polar symmetry, the displacement field is independent of θ, and $s_\theta = 0$. Hence, according to the Lagrange-Kirchhoff model, the non-zero component of strain are the radial $\varepsilon_r(r, z, t)$ and the circumferential one $\varepsilon_\theta(r, z, t)$. That is,

$$\varepsilon_r = \partial_r s_r = -z\,\partial_r^2 w = z\,\chi_r \tag{2a}$$

$$\varepsilon_\theta = \frac{s_r}{r} = -\frac{z}{r}\partial_r w = z\,\chi_\theta \tag{2b}$$

where $\chi_r(r, t)$ and $\chi_\theta(r, t)$ are the radial and circumferential bending curvatures, respectively.

2.2 Indefinite equilibrium equations

The indefinite equilibrium equations of the circular plate in polar coordinates under axisymmetric assumptions are obtained considering the infinitesimal plate element shown in Fig. 1. In dynamic conditions, under the assumption that the rotational effects related to the inertial forces are negligible, the equilibrium equations are

$$\partial_r T_r + \frac{T_r}{r} = \rho_h \partial_t^2 w - q \tag{3a}$$

$$\partial_r M_r + \frac{M_r - M_\theta}{r} = T_r \tag{3b}$$

where $q(r, t)$ is the load per unit area acting in vertical direction z, $T_r(r, t)$ is the shear forces flow, $M_r(r, t)$, $M_\theta(r, t)$ are bending moment flows, $\rho_h = \rho\, h$ is the mass density per unit of area of the plate. The involved force and moment flows are defined as

$$T_r(r, t) = \int_{-h/2}^{h/2} \tau_{rz} dz, \qquad M_r(r, t) = \int_{-h/2}^{h/2} \sigma_r\, z\, \mathrm{d}z, \qquad M_\theta(r, t) = \int_{-h/2}^{h/2} \sigma_\theta\, z dz \tag{4}$$

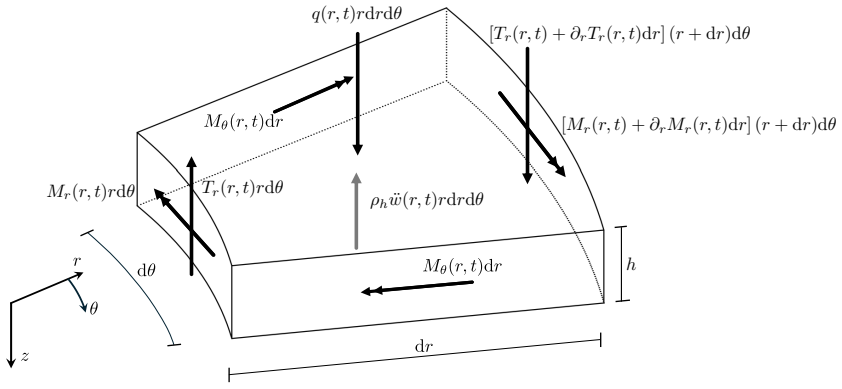

Figure 1: Free body diagram of infinitesimal plate element

where $\tau_{rz}(r,z,t)$ is the shear stress acting in vertical direction z on the faces of the plate volume element normal to r, $\sigma_r(r,z,t)$ and $\sigma_\theta(r,z,t)$ are the normal stress along r and θ, respectively. Eqs. (3) can be combined to obtain a single partial differential equation governing the dynamic equilibrium. That is,

$$\partial_r^2 M_r + \frac{2}{r}\partial_r M_r - \frac{1}{r}\partial_r M_\theta = \rho_h \partial_t^2 w - q \tag{5}$$

2.3 Time-dependent nonlocal constitutive law

The nonlocal constitutive law is derived starting from the viscoelastic local one.

2.3.1 Local fractional-order viscoelasticity

Various isotropic homogeneous linear time-dependent stress-strain models lead to the following relations in terms of bending moment flow and curvature

$$\mathbb{D}_t\left[\chi_r(r,t)\right] = \frac{M_r(r,t) - \nu M_\theta(r,t)}{(1-\nu^2)} \tag{6a}$$

$$\mathbb{D}_t\left[\chi_\theta(r,t)\right] = \frac{M_\theta(r,t) - \nu M_r(r,t)}{(1-\nu^2)} \tag{6b}$$

where $\mathbb{D}_t\left[\cdot\right]$ is a linear time-dependent differential operators related to the chosen viscoelastic model. Among the viscoelastic models we consider the fractional order Kelvin-Voigt, where the differential operator is

$$\mathbb{D}_t\left[f(t)\right] = \mathcal{D}\left(1 + \tilde{t}^\beta \partial_t^\beta\right) f(t) \tag{7}$$

$\mathcal{D}$ represents the bending stiffness of the plate

$$\mathcal{D} = \frac{E\,h^3}{12(1-\nu^2)} \tag{8}$$

being E the Young modulus and ν the Poisson's ratio, $\tilde{t}$ is a characteristic time, such that the viscosity of the material is expressed as $\mu = E\,\tilde{t}$, $\beta \in [0,\,1]$ is the fractional order of the involved Caputo's

fractional derivative ∂_t^β, which is defined as follows

$$\partial_t^\beta f(t) := \begin{cases} \dfrac{1}{\Gamma(1-\beta)} \displaystyle\int_0^t (t-\bar{t})^{-\beta}\, \partial_{\bar{t}} f\,(\bar{t})\, \mathrm{d}\bar{t} & \text{if } 0 \leqslant \beta < 1 \\ \\ \partial_t f(t) & \text{if } \beta = 1 \end{cases} \tag{9}$$

$\Gamma(\cdot)$ is the Euler gamma function. It is worth noting that classic Kelvin-Voigt model can be seen as a special case when $\beta = 1$ and Elastic relation can be obtained placing $\tilde{t}^\beta \to 0$.

The adopted fractional-order time-dependent model leads to the following local bending moment flux-curvature relation

$$\left(1 + \tilde{t}^\beta \partial_t^\beta\right) \chi_r(r,t) = \frac{M_r(r,t) - \nu M_\theta(r,t)}{\mathcal{D}(1-\nu^2)} \tag{10a}$$

$$\left(1 + \tilde{t}^\beta \partial_t^\beta\right) \chi_\theta(r,t) = \frac{M_\theta(r,t) - \nu M_r(r,t)}{\mathcal{D}(1-\nu^2)} \tag{10b}$$

2.3.2 Stress-driven nonlocal model

According to the integral stress-driven formulation [13], and taking into account the axisymmetry of the problem we assume that the nonlocal curvature $\boldsymbol{\chi}_r(r,t)$ is a function of the entire local one $\chi_r(r,t)$ by the following Fredholm convolution integral

$$\boldsymbol{\chi}_r(r,t) = (\phi_\lambda * \chi_r) = \int_{-R}^{R} \phi_\lambda(r-\bar{r}) \chi_r(\bar{r},t) \mathrm{d}\bar{r} \tag{11}$$

the averaging kernel $\phi_\lambda(r)$ must have the properties of positivity, symmetry, normalization and limit impulsivity. In this study, the Helmotz bi-exponential kernel is selected. That is,

$$\phi_\lambda(r) = \frac{1}{2\mathcal{R}_\lambda} \exp\left(-\frac{|r|}{\mathcal{R}_\lambda}\right) \tag{12}$$

where $\mathcal{R}_\lambda = \lambda R$, and λ is the dimensionless nonlocal parameter. This specific choice of the nonlocal kernel allows us to recast the nonlocal integral formulation into an equivalent differential form, supplemented with appropriate constitutive boundary conditions (CBCs). Specifically, the integral relation in Eq. (11) is equivalent to the following differential problem

$$\begin{cases} -\mathcal{R}_\lambda^2\, \partial_r^2 \boldsymbol{\chi}_r + \boldsymbol{\chi}_r = \chi_r \\ \\ \text{CBCs} \begin{cases} \mathcal{R}_\lambda \partial_r \boldsymbol{\chi}_r = \boldsymbol{\chi}_r & \text{in } r = -R \\ \mathcal{R}_\lambda \partial_r \boldsymbol{\chi}_r = -\boldsymbol{\chi}_r & \text{in } r = R \end{cases} \end{cases} \tag{13}$$

2.3.3 Bending viscoelastic nonlocal model

By combining time-dependent viscoelastic relation in Eq. (10) and the nonlocal differential formulation in Eq. (13), the flux bending moments are given as

$$M_r(r,t) = \mathcal{D}\left(1+\tilde{t}^{\beta}\partial_t^{\beta}\right)\left(\boldsymbol{\chi}_r + \nu\boldsymbol{\chi}_\theta - \mathcal{R}_\lambda^2\,\partial_r^2\boldsymbol{\chi}_r\right) \tag{14a}$$

$$M_\theta(r,t) = \mathcal{D}\left(1+\tilde{t}^{\beta}\partial_t^{\beta}\right)\left(\boldsymbol{\chi}_\theta + \nu\boldsymbol{\chi}_r - \mathcal{R}_\lambda^2\,\partial_r^2\boldsymbol{\chi}_\theta\right) \tag{14b}$$

It is worth noting that the local elastic and viscoelastic cases are particular instances of these more general constitutive relations in terms of bending flow moments and curvature. For example, the local cases are recovered when $\lambda \to 0$. The nonlocal differential relations in Eqs. (14) must always be accompanied by the CBCs in Eq. (13).

2.4 Equilibrium equation of nonlocal viscoelastic Kirchoff-Lagrange plate

By substituting the nonlocal viscoelastic bending relations in Eqs.(14) into the equilibrium equation (5), and by taking into account the kinematic relations in Eqs.(2), the governing equation becomes

$$\mathcal{D}\left(1+\tilde{t}^{\beta}\partial_t^{\beta}\right)\left[\nabla_r^4 w - \mathcal{R}_\lambda^2\left(\partial_r^6 w + \frac{2-\nu}{r}\partial_r^5 w\right)\right] + \rho_h\partial_t^2 w = q \tag{15}$$

where $\nabla_r^4 w$ denotes the biharmonic operator in cylindrical coordinates for the axisymmetric case. That is,

$$\nabla_r^4 w(r,t) = \partial_r^4 w(r,t) + \frac{2}{r}\partial_r^3 w(r,t) - \frac{1}{r^2}\partial_r^2 w(r,t) + \frac{1}{r^3}\partial_r w(r,t) \tag{16}$$

The solution in terms of $w(r,t)$ of Eq. (15) can be found by imposing two initial conditions, four mechanical/kinematic boundary conditions and the two CBCs in Eqs. (13).

3 FREQUENCY ANALYSIS FOR STOCHASTIC EXCITATIONS

Eq. (15) can be solved by assuming the separation of the variable and performing the continuous modal analysis. However, for the non-local cases ($\lambda > 0$) the eigen-functions cannot be evaluated in closed form. For this reason the eigen-analysis is conducted below by discretizing the spatial domain into finite elements and evaluating the eigenvectors of the problem. Specifically, the space-variable $r \in [R, -R]$ is divided in a finite number n of spatial elements of length $\Delta r = 2R/n$ such that $r_j = j\Delta r$, where j is an integer number varying in the interval $[-n/2, n/2]$. In this way the approximate solution of the displacement function $w(r,t)$ can be obtained in terms of the displacement time-dependent vector $\mathbf{w}(t)$ composed by $n+1$ functions such that $\mathrm{w}_j(t) \approx w(j\Delta r, t)$. By this approach the partial differential equation in Eq. (15) leads to the following set of coupled differential equations

$$\mathbf{K}\left[\mathbf{w}(t) + \tilde{t}^{\beta}\partial_t^{\beta}\mathbf{w}(t)\right] + \mathbf{M}\,\ddot{\mathbf{w}}(t) = q(t)\mathbf{p} \tag{17}$$

being $\mathbf{K}$ the stiffness matrix obtained by performing the central difference of the differential operator in the square brackets in Eq. (15), $\mathbf{M}$ is a diagonal mass matrix, where each term is $m_{jj} = \rho_h$, $\mathbf{p}$ is the influence vector that describes loading space-distribution and $q(t)$ is time-dependent part of the load. In the following, we assume that the load function has a deterministic spatial distribution and a stochastic temporal evolution.

3.1 Modal transformation

The dynamic analysis can be conveniently carried out by introducing the following modal transformation

$$\mathbf{w}(t) = \mathbf{\Phi}\,\mathbf{y}(t) \tag{18}$$

where $\mathbf{y}(t)$ is the vector of the modal coordinates, and $\mathbf{\Phi}$ is the matrix of eigenvectors of dynamic matrix $\mathbf{D} = \mathbf{K}^{-1}\mathbf{M}$. By performing this modal transformation Eq. (17) yields

$$\mathbf{\Phi}^{-1}\mathbf{\Phi}\left[\mathbf{y}(t) + \tilde{t}^{\beta}\partial_t^{\beta}\mathbf{y}(t)\right] + \mathbf{\Phi}^{-1}\mathbf{D}\mathbf{\Phi}\,\ddot{\mathbf{y}}(t) = \mathbf{\Phi}^{-1}\mathbf{K}^{-1}\mathbf{p}\,q(t) \tag{19}$$

by introducing the diagonal matrix $\mathbf{\Gamma} = \mathbf{\Phi}^{-1}\mathbf{D}\mathbf{\Phi}$ and the vector $\tilde{\mathbf{p}} = \mathbf{\Phi}^{-1}\mathbf{K}^{-1}\mathbf{p}$, the system of uncoupled fractional-order differential equations governing the motion of n modal oscillators takes the form

$$\mathbf{y}(t) + \tau^{\beta}\partial_t^{\beta}\mathbf{y}(t) + \mathbf{\Gamma}\,\ddot{\mathbf{y}}(t) = \tilde{\mathbf{p}}\,q(t) \tag{20}$$

each modal coordinate $y_j(t)$ can be obtained by solving the differential equation

$$y_j(t) + \tilde{t}^{\beta}\partial_t^{\beta}y_j(t) + \gamma_j\ddot{y}_j(t) = \tilde{p}_j q(t) \tag{21}$$

by introducing the modal damping factor ξ_j and the angular frequency $\tilde{\omega}_j = \sqrt{1/\gamma_j}$, the Eq. (21) can be rewritten in canonical form as

$$\tilde{\omega}_j^2 y_j(t) + 2\xi_j\tilde{\omega}_j^{2-\beta}\partial_t^{\beta}y_j(t) + \ddot{y}_j(t) = \bar{p}_j q(t) \tag{22}$$

where $\bar{p}_j = \tilde{p}_j/\gamma_j$. Frequency analysis can be carried out by applying the Fourier transform to Eq. (21). Accordingly,

$$\hat{y}_j(\omega, T)\left\{\tilde{\omega}_j^2\left[1 + 2\xi_j\left(i\,\frac{\omega}{\tilde{\omega}_j}\right)^{\beta}\right] - \omega^2\right\} = \bar{p}_j\hat{q}(\omega, T) \tag{23}$$

where $\hat{y}_j(\omega, T)$ and $\hat{q}(\omega, T)$ indicates the truncated Fourier transform in a finite time interval $[0, T]$ of the process $y_j(t)$ and $q(t)$, respectively.

3.2 Spectral analysis

Now we turn our attention to the random vibrations of the viscoelastic nonlocal plate, assuming that the time-dependent part of the transverse load $q(t)$ is a stationary Gaussian white noise with zero mean denoted by $\eta(t)$. It is characterized by a Dirac delta as characteristic function (CF). That is,

$$R_{\eta}(\bar{t}) = \mathbb{E}\left[\eta(t)\eta(t + \bar{t})\right] = 2\pi S_0\delta\left(\bar{t}\right) \tag{24}$$

where $\mathbb{E}[\cdot]$ is the averaging operator. Being $\eta(t)$ a stationary process, by virtue of Wiener-Khinchin theorem, the power spectral density (PSD), denoted by $S_{\eta}(\omega)$, is the Fourier transform of the CF. That is,

$$S_{\eta}(\omega) := \frac{1}{2\pi}\int_{-\infty}^{\infty} R_{\eta}(\bar{t})e^{-i\omega\bar{t}}\mathrm{d}\bar{t} = \lim_{T\to\infty}\frac{1}{2\pi T}\mathbb{E}\left[\hat{\eta}^{*}(\omega, T)\hat{\eta}(\omega, T)\right] = S_0 \tag{25}$$

where $i = \sqrt{1}$ is the imaginary unit, $\hat{\eta}^{*}(\omega, T)$ denotes the complex conjugate of $\hat{\eta}(\omega, T)$.

A complete characterization of the stationary response of the nonlocal viscoelastic plate can be obtained by the evaluation of the PSD matrix $\mathbf{S}_{\mathbf{w}}(\omega)$ of $\mathbf{w}(t)$. Taking into account the modal transformation in Eq. (18) that PSD matrix is

$$\mathbf{S}_{\mathbf{w}}(\omega) = \lim_{T\to\infty} \frac{1}{2\pi T}\mathbb{E}\left[\hat{\mathbf{w}}^*(\omega,T)\hat{\mathbf{w}}^{\mathrm{T}}(\omega,T)\right] = \mathbf{\Phi}\mathbf{S}_{\mathbf{y}}(\omega)\mathbf{\Phi}^{\mathrm{T}} \tag{26}$$

where $\mathbf{S}_{\mathbf{y}}(\omega)$ is the PSD matrix of the modal coordinate vector $\mathbf{y}(t)$, defined as

$$\mathbf{S}_{\mathbf{y}}(\omega) = \lim_{T\to\infty} \frac{1}{2\pi T}\mathbb{E}\left[\hat{\mathbf{y}}^*(\omega,T)\hat{\mathbf{y}}^{\mathrm{T}}(\omega,T)\right] \tag{27}$$

where $\hat{\mathbf{y}}(\omega,T)$ can be obtained by performing the Fourier transform of the Eq. (20), that is,

$$\left\{\left[1+\left(i\omega\tilde{t}\right)^{\beta}\right]\mathbf{I}-\omega^2\mathbf{\Gamma}\right\}\hat{\mathbf{y}}(\omega,T) = \tilde{\mathbf{p}}\,\hat{\eta}(\omega,T) \tag{28}$$

where $\mathbf{I}$ is the identity matrix. By Eq. (28) $\hat{\mathbf{y}}(\omega,T)$ can be obatined as

$$\hat{\mathbf{y}}(\omega,T) = \mathbf{H}(\omega)\,\hat{\eta}(\omega,T) \tag{29}$$

being the diagonal transfer function $\mathbf{H}(\omega) = \left\{\left[1+\left(i\omega\tilde{t}\right)^{\beta}\right]\mathbf{I}-\omega^2\mathbf{\Gamma}\right\}^{-1}\tilde{\mathbf{p}}$. According to Eq. (23) j-th diagonal term of $\mathbf{H}(\omega)$, denoted as $H_{jj}(\omega)$, is given as

$$H_{jj}(\omega) = \frac{\bar{p}_j}{\tilde{\omega}_j^2\left[1+2\xi_j\left(i\,\omega/\tilde{\omega}_j\right)^{\beta}\right]-\omega^2} \tag{30}$$

By taking into account Eqs. (25), (26), (27) and (29), the PSD matrix of $\mathbf{w}(t)$ is given as

$$\mathbf{S}_{\mathbf{w}}(\omega) = S_{\eta}(\omega)\mathbf{\Phi}\mathbf{H}^*(\omega)\mathbf{H}^{\mathrm{T}}(\omega)\mathbf{\Phi}^{\mathrm{T}} = S_0\mathbf{\Phi}\mathbf{H}^*(\omega)\mathbf{H}^{\mathrm{T}}(\omega)\mathbf{\Phi}^{\mathrm{T}} \tag{31}$$

the generic term of the PSD matrix, denoted as $S_{\mathrm{w}_j\mathrm{w}_k}(\omega)$, represents the cross-PSD between the process $\mathrm{w}_j(t)$ and $\mathrm{w}_k(t)$. That is,

$$S_{\mathrm{w}_j\mathrm{w}_k}(\omega) = \lim_{T\to\infty} \frac{1}{2\pi T}\mathbb{E}\left[\hat{\mathrm{w}}_j^*(\omega,T)\hat{\mathrm{w}}_k(\omega,T)\right] \tag{32}$$

From PSD matrix the covariance one $\mathbf{\Sigma}_{\mathbf{w}}$ can be evaluated as

$$\mathbf{\Sigma}_{\mathbf{w}} = \int_{-\infty}^{\infty}\mathbf{S}_{\mathbf{w}}(\omega)\mathrm{d}\omega \tag{33}$$

this matrix contains variance and cross-variance of the response, e.g., its generic term σ_{jk}^2 represents the stationary cross-variance between the process $\mathrm{w}_j(t)$ and $\mathrm{w}_k(t)$ defined as

$$\sigma^2_{\mathrm{w}_j\mathrm{w}_k} = \int_{-\infty}^{\infty} S_{\mathrm{w}_j\mathrm{w}_k}(\omega)\mathrm{d}\omega \tag{34}$$

when $j=k$ the PSD and variance will be indicate as $S_{\mathrm{w}_j}(\omega)$ and $\sigma^2_{\mathrm{w}_j}$, respectively.

4 NUMERICAL RESULTS AND PARAMETRIC ANALYSIS

For the numerical simulations, we consider a simply supported circular plate with the geometrical and mechanical parameters listed in Table 1. The mechanical parameters refer to an elastomer used as a dielectric in structural elements of WEC devices (*Silopren LSR 2740 TP3783*). The plate is subjected to a uniformly distributed load with a time-varying amplitude modeled as a zero-mean Gaussian white noise process with $S_0 = 1.00\,\mathrm{s}$. The numerical solution was obtained by dividing the domain into n elements. The maximum deflection occurs at $r = 0$, which corresponds to the $1 + n/2$-th entry of the vector $\mathbf{w}(t)$, that is, $\mathrm{w}_{31}(t) \approx w(0,t)$. This discretization was performed so as to ensure an error of approximately $2\,\%$ on the fourth peak of the PSD of the maximum displacement, with respect to the analytical solution based on known eigenfunctions of the local case as $\lambda \to 0$. For the maximum displacement, PSD analysis is presented below, including the evaluation of the stationary variance and peak frequencies, by varying both viscoelastic β and nonlocal parameter λ.

R [m]	h [m]	n	Δr [m]	E [Pa]	$\tilde{t}$ [s]	β	μ [Pa s]	ρ [kg/m^3]	ν
1.00	0.07	60	$16.67 \cdot 10^{-3}$	$9.00 \cdot 10^{6}$	$6.77 \cdot 10^{-5}$	1.00	610.00	1120.00	0.50

Table 1: Geometrical and mechanical parameters of the circular plate

First, the PSD of the maximum deflection $S_{\mathrm{w}_{31}}(\omega)$ is shown in Fig. 2 for the local viscoelastic case $\lambda \to 0$ and different values of the viscoelastic parameters β. It can be observed that the peak frequencies shift to higher values as β decreases. This behavior can be explained by noting that the fractional Kelvin–Voigt model becomes increasingly elastic for smaller values of β. Moreover, the amplitude of the peaks increases with increasing values of β. A similar trend with respect to variations in the viscoelastic parameter β is observed in Fig. 3 for the nonlocal case where $\lambda = 0.05$. However, by comparing the first two Figures, it is evident that the peak frequencies increase in the nonlocal case, while the maximum amplitudes decrease. This is because the adopted nonlocal model leads to an increase in both the stiffness and viscosity, and thus in the damping, of the material as λ increases. Finally, Fig. 4 shows the comparison among the PSDs obtained for different values

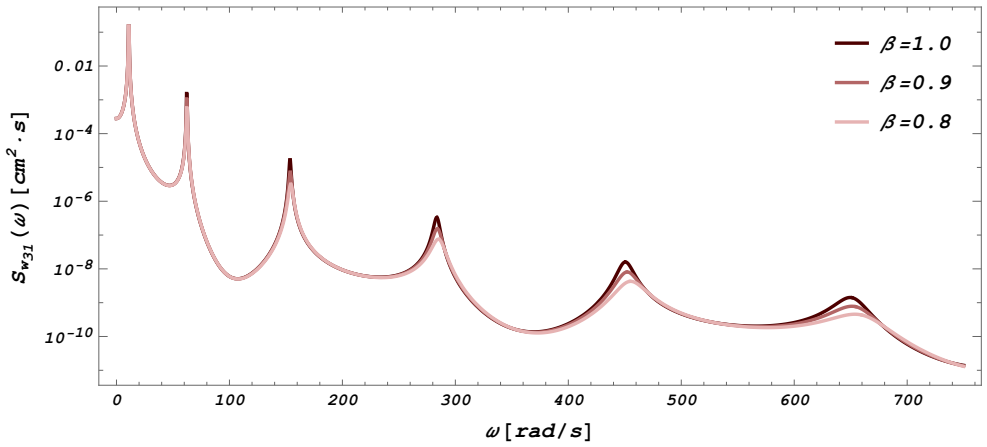

Figure 2: PSD of $\mathrm{w}_{31}(t)$ for the local case $\lambda \to 0$ and different value of viscoelastic parameter β

of λ, with $\beta = 1$ fixed (classic Kelvin-Voigt model). It can be observed that the PSD peaks shift to higher frequencies as λ increases, while their amplitudes decrease accordingly. This behavior is

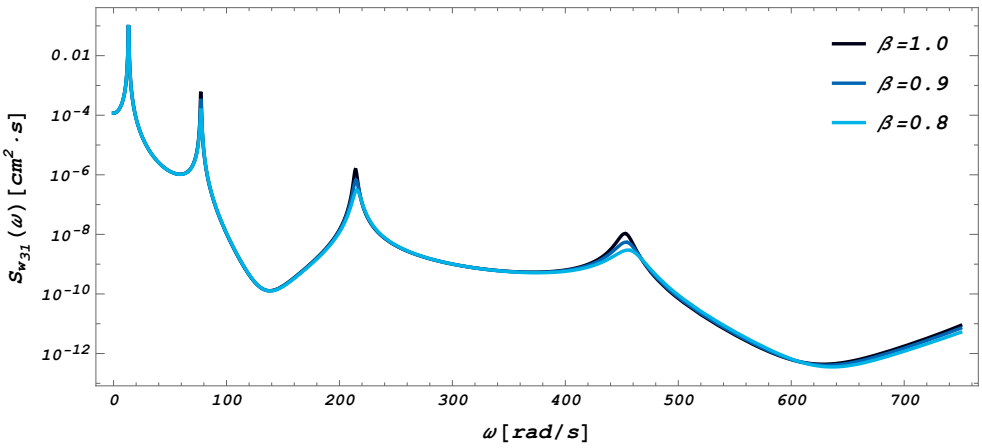

Figure 3: PSD of $\mathrm{w}_{31}(t)$ for the nonlocal case $\lambda = 0.05$ and different value of viscoelastic parameter β

consistent with the well-known stiffness effect induced by nonlocal interactions in the stress-driven nonlocal model [25], which becomes more pronounced for larger values of λ. Numerical variations

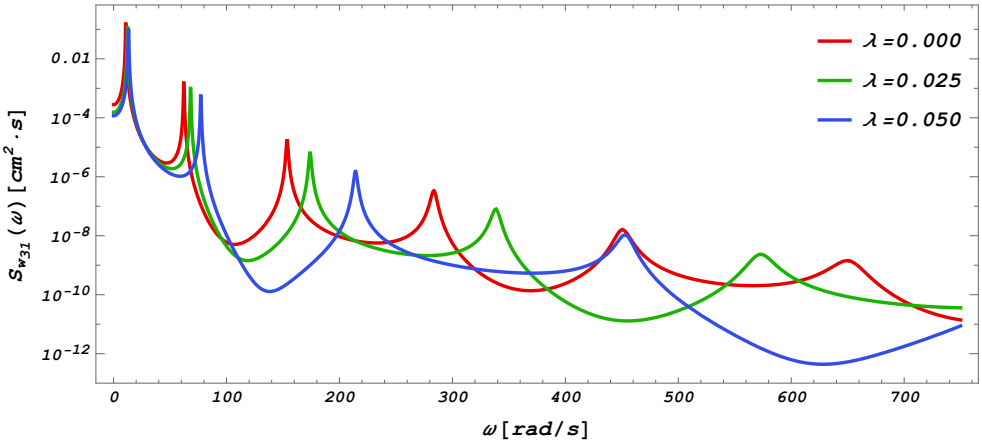

Figure 4: PSD of $\mathrm{w}_{31}(t)$ for different values of the nonlocal parameter λ for $\beta = 1$

of the peak frequencies and the variances of the maximum deflection are reported in the Table 2 as a function of the nonlocal parameter.

5 CONCLUSIONS

A mechanical model has been proposed to describe the dynamic behavior of a circular thin nonlocal viscoelastic plate. Main concluding remarks are reported below.

- The model accounts for nonlocal effects to represent spatial long-range interactions and incorporates fractional viscoelasticity to characterize the time-dependent behavior of rheological materials.

- The resulting well-posed problem is formulated as a sixth-order differential equation, accompanied by four kinematic/mechanical boundary conditions, two constitutive boundary conditions, and two initial conditions.

- The numerical results highlight the sensitivity of the structural frequency response to key mechanical parameters—particularly the nonlocal parameter and the fractional-order viscoelastic coefficient—emphasizing their influence on peak frequencies and displacement variance.

λ	ω_1 [rad/s]	ω_2 [rad/s]	ω_3 [rad/s]	ω_4 [rad/s]	$\sigma^2_{w_{31}}$ [cm^2]
0.000	10.88	62.45	153.64	283.61	13.45
0.025	12.50	68.23	173.98	338.52	7.44
0.050	13.25	77.30	214.23	452.78	5.63

Table 2: Peak frequencies and stationary variance of the maximum deflection for $\beta = 1$ and different value of λ.

Acknowledgments

Study financed by the EU – Next-GenerationEU – PNRR– MISS. 4 COMP. 2, INVEST. N. 1.1, BANDO PRIN 2022 D.D. 104 of 02-02-2022. F.P. Pinnola and F. Scudieri gratefully acknowledge the financial support received from the Project 2022TMSPLS - *TUNed Dampers Exploitation to Raise VIBration Energy harvesting* TUNDERVIBE (CUP N. E53D23003740006). F. Marotti de Sciarra gratefully acknowledges the financial support received from the Proj. 2022X5L45T *Preparation and Performances of PCs with Nanostructures for Civil Eng. Projects* (CUP N. E53D23003860006).

REFERENCES

[1] Eringen AC. Linear theory of nonlocal elasticity and dispersion of plane waves. *Int J Eng S*, 10:425–435, 1972.

[2] Eringen AC. On differential equations of nonlocal elasticity and solutions of screw dislocation and surface waves. *J Appl Phys*, 54:4703, 1983.

[3] Challamel N and Wang CM. The small length scale effect for a non-local cantilever beam: a paradox solved. *Nanotechnology*, 19:345703, 2008.

[4] Loya JA Reddy JN Fernández-Sáez J, Zaera R. Bending of euler–bernoulli beams using eringen's integral formulation: a paradox resolved. *Int J Eng Sci*, 99:107–116, 2016.

[5] Borino G, Failla B, and Parrinello F. A symmetric nonlocal damage theory. *Int J Solids Struct*, 40:3621–3645, 2003.

[6] Polizzotto C, Fuschi P, and Pisano AA. A strain-difference-based nonlocal elasticity model. *Int J Solids Struct*, 41:2383–2401, 2004.

[7] Apuzzo A, Barretta, Faghidian SA, Luciano R, and Marotti de Sciarra F. Free vibrations of elastic beams by modified nonlocal strain gradient theory. *Int J Eng Sci*, 133:99–108, 2008.

[8] Lakes R. Experimental micro mechanics methods for conventional and negative poisson's ratio cellular solids as cosserat continua. *J Eng Mater-T ASME*, 113(1):148–155, 1991.

[9] Mindlin RD. Influence of couple-stresses on stress concentrations. *Exp Mech*, 3(1):1–7, 1963.

[10] Silling SA. Reformulation of elasticity theory for discontinuities and long-range forces. *J Mech Phys Solids*, 48(1):175–209, 2000.

[11] Zingales M Di Paola M, Pirrotta A. Mechanically based approach to non-local elasticity: variational principles. *Int J Solids Struct*, 47(5):539–548, 2010.

[12] Alotta G, Di Paola M, and Pinnola FP. An unified formulation of strong non-local elasticity with fractional order calculus. *Meccanica*, 57(4):793–805, 2022.

[13] G. Romano, R. Barretta, M. Diaco, and F. Marotti de Sciarra. Constitutive boundary conditions and paradoxes in nonlocal elastic nanobeams. *Int J Mech Sci*, 121:151–156, 2017.

[14] Romano G and Barretta R. Nonlocal elasticity in nano beams: the stress-driven integral model. *Int J Eng Sci*, 115:14–27, 2017.

[15] Nutting PG. A new general law of deformation. *J Franklin Inst*, 191:679–685, 1921.

[16] Podlubny I. Fractional differential equation. *Academic Press, San Diego*, 191:679–685, 1999.

[17] Di Paola M, Pirrotta A, and Valenza A. Visco-elastic behavior through fractional calculus: an easier method for best fitting experimental results. *Mech Mater*, 43:799–806, 2011.

[18] Pedram O Rahmani O. Analysis and modeling the size effect on vibration of functionally graded nanobeams based on nonlocal timoshenko beam theory. *Int J Eng Sci*, 77:55–70, 2014.

[19] Bažant ZP. Mechanics of distributed cracking. *Appl Mech Rev*, 39(5):675–705, 1986.

[20] Wang L and Hu H. Flexural wave propagation in single-walled carbon nanotubes. *Phys Rev B COndens Matter Mater Phys*, 71(19):195412, 2005.

[21] Alotta G, Failla G, and Pinnola FP. Stochastic analysis of a nonlocal fractional viscoelastic bar forced by gaussian white noice. *Finite Elem Anal Des*, 3(3):030904, 2017.

[22] Alotta G, Failla G, and Zingales M. Finite element method for a nonlocal timoshenko beam model. *Finite Elem Anal Des*, 89:77–92, 2014.

[23] Dorfmann L and Ogden R W. Nonlinear electroelasticity: material properties, continuum theory and applications. *Proc R Soc A*, 473:20170311, 2017.

[24] Rosati Papini GP, Moretti G, Vertechy R, and Fontana M. Control of an oscillating water column wave energy converter based on dielectric elastomer generator. *Nonlinear Dyn*, 92:181–202, 2018.

[25] Pinnola FP, Vaccaro MS, Barretta R, and Marotti de Sciarra F. Random vibrations of stress-driven nonlocal beams with external damping. *Meccanica*, 56(6):1329–1344, 2021.

[26] Vaccaro SM, Pinnola FP, Marotti de Sciarra F, Canadija M, and Barretta R. Stress-driven two-phase integral elasticity for timoshenko curved beams. *Proc. Inst. Mech. Eng., Part N*, 235 (1-2):52–63, 2021.

[27] Pinnola FP, Vaccaro MS, Barretta R, and Marotti de Sciarra F. Finite element method for stress-driven nonlocal beams. *Engineering Analysis with Boundary Elements*, 134:22–34, 2022.

[28] Alotta G, Russillo Af, and Failla G. Elastic wave propagation in periodic stress-driven nonlocal timoshenko beams. *Int J Solids Struct*, 306:113103, 2025.